Effect of phases on the energetics of pristine InP nanowires: An *ab-initio* approach

Pankaj Srivastava[1*], Avaneesh Kumar[1], Neeraj K. Jaiswal[2] , Varun Sharma[1]

[1]*Nanomaterials Research Group, ABV-Indian Institute of Information Technology and Management (IIITM),
Gwalior 474015, India*
[2]*Discipline of Physics, Indian Institute of Information Technology, Design and Manufacturing (IIITDM),
Jabalpur 482005, India*

[*]Corresponding author. Tel: (+91) 751-2449814; E-mail: pankajs@iiitm.ac.in

ABSTRACT

We have investigated the electronic and structural properties of pristine Zinc-blende type InP nanowires (NWs) by using *ab-initio* approach. We have considered the effect of phases by taking NWs of 7 Å radii in three phases viz. (100), (110), (111). It is revealed that the electronic properties of NWs are highly affected by the wire phases. NW in (100) phase is found to be semiconducting with an indirect band gap of 0.71 eV whereas it becomes semi-metallic and metallic in other two phases. Thus, the nature of nanowires is observed as a function of NW phases. Further, energetic feasibility of InP NWs strongly dependent on their growth phase. Copyright © 2016 VBRI Press.

Keywords: Semiconductor nanowire; *ab-initio* calculation; DFT; electronic properties; zinc-blende.

Introduction

In recent years, researchers have shown keen interest towards the study of nanoscale semiconductor structure because of their unique properties compared to its bulk counterpart. Especially one–dimensional nanowires (NWs), which play significant role in the future nanoscale application by acting as basic building blocks for fabrication of nanoscale devices [1, 2, 3]. Past experiment had proved already that semiconducting NWs can be used as building blocks of various electronic devices, including transistors [4, 5, 6], sensors [7, 8] as well as p-n diode [9, 10]. InP NWs emerged out as a favorable material for next generation optical based application [1, 2, 9]. Premila *et al.* [11] systematically grow InP NWs arrays by using catalyst-free selective area metalorganic vapour phase epitaxy method. Mark *et al.* [12] synthesized InP NWs using laser catalytic growth (LCG) process and developed a method to control precisely the diameter and length of NWs. Their study also implies that InP NWs can be favorably grown along (111) direction. Whereas, Dayne *et al.* [13] synthesis high crystalline zinc blende (ZB) GaP, GaAs and InP NWs using solution−liquid−solid (SLS) method with the help of Bi nanocrystals acting as crystallization seeds. Yang *et al.* [14] synthesized InP and GaP NWs from Ullmann- like reaction. The results from energy dispersive x-ray spectroscopy (EDS) and high-resolution transmission electron microscopy (HRTEM) images show that the prepared NWs were having sphalerite structure. Similarly Hannah *et al.* [15] synthesize high-quality Zinc-blende (ZB) and Wurtzite (WZ) III-V group NWs by controlling the basic growth temperature and V/III ratio parameters. Branched InP NWs is also synthesized by using solvothermal technique [16]. Results suggest that synthesized NWs are in cubic phase with lattice constant of 5.858Å.

Various theoretical work of semiconductor NWs has also been reported in the recent past. Claudia *et al.* [17] investigated the influence of mechanical strain on electronic behavior of InP and InAs NWs. Sano *et al.* [18] analyzed the twinning formation of InP NWs using Monte-Carlo simulation. Akiyama *et al.* [19] observed a ZB to WZ phase transition in InP NWs as the width of NWs reduces. Leitsmann *et al.* [20] analyzed that surface structure control the energetics of hexagon-shaped [111]/[0001] directed III-V semiconductor nanorods. Gadret *et al.* [21] experimentally analyze the valence-band splitting energies of WZ InP NWs using photoluminescence excitation technique. Their theoretical results based on *ab-initio* calculation are in good agreement with the experimental results. Yamashita *et al.* [22] reported that facet orientation is an important key parameter to determine the stability and crystal structural of III-V NWs. Apart from these experimental and theoretical investigations, little is so far known about the influence of different crystallographic phase of growing III-V group NWs. Most reports are related to the dimensional dependent structural stability of NWs. Therefore, it is important to understand the effects of different crystallographic phase on the energetic of NWs. In the present work, we perform a comprehensive theoretical study to investigate the effect of phases on energetic of pristine InP NWs using *ab-initio* approach.

Experimental

Present calculations were performed with the Vienna *ab-initio* Simulation Package (VASP) [23, 24] under the framework of density functional theory (DFT) within local-

density approximation (LDA) [25] to described exchange-correlation energy of electrons. Projector augmented wave method (PAW) [26] is used to define interaction between ionic core and valance electrons. Plane wave expansion of upto 320 eV cut-off energy was used for calculation. For benchmark calculation, we calculated structural and electronic properties of bulk ZB InP. Brillouin-zone of the bulk InP is sampled using $1\times1\times5$ k-points mesh using Monkhorst-pack scheme [27], resulting $10k$- points in the irreducible Brillouin zone (IBZ). Based on optimized InP bulk structure, we modeled pristine InP NWs along three different phases (100), (110) and (111). All the NW geometry are considered roughly spherical. For structural optimization $1\times1\times5$ k-points mesh is used, resulting $3k$-points in the IBZ of NW supercell. The periodicity of all NWs was maintained along the z-axis. The structures were optimized until forces on each atom are below 0.05 eVÅ^{-1} and convergence criteria for energy is taken to be 10^{-3} eV. A vacuum space 10 Å is also modelled along x and y-axis to avoid interactions between NWs and their periodic images.
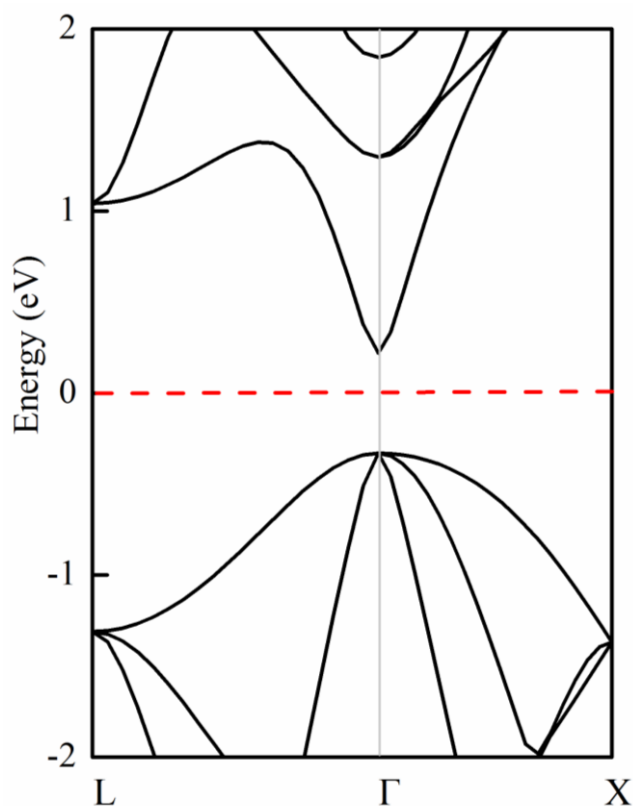

Fig. 1. Band Structures of Zinc-blend Bulk InP. The Fermi level is set at 0 eV as shown by dashed line.

Results and discussion

For benchmark purpose, we obtain the electronic and structural properties of bulk ZB InP and compare them with existing data. The computed lattice constant and energy band-gap **[Fig. 1]** for ZB bulk InP is 5.877Å and 0.55eV, which is in good agreement with other reported experimental and theoretical work shown as in **Table 1**.

However, our calculated energy band-gap is smaller than experimental reported value. This underestimation of band-gap is due to a well-known limitation of DFT calculation.
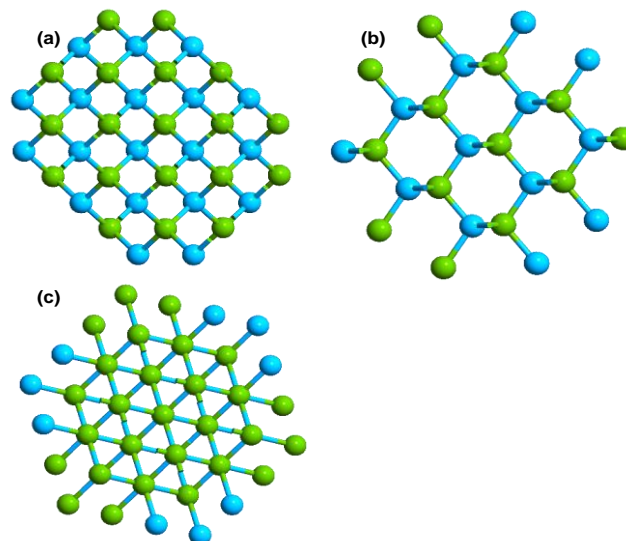
Fig. 2. Schematic top view of pristine 7Å radius NWs in (a) (100), (b) (110), (c) (111) phases. Where green and sky blue balls represent P and in atoms respectively.

Obtained ZB bulk InP structure is used to modelled the unit cell of NWs structure, which are directed along (100), (110), and (111) phases contain 38, 48, and 56 atoms for 7Å radii respectively as shown in **Fig. 2** (**a**), (**b**) and (**c**). On analysing the relaxed NWs structure, it is found that In-P bond undergo strong modification after complete optimization of NWs. Bond length ranges from 2.47 Å to 2.60 Å, 2.5 Å to 2.71 Å, 2.48Å to 2.68 Å for the NWs directed along (100), (110), and (111) phases respectively. Average bond length of surface atoms is 2.582 Å and core atoms are 2.518 Å.

Table. 1. Calculated lattice constant and Energy band-gap compared to other work of Zinc-Blende InP bulk.

Parameter	Our work	Theoretical		Experimental
Exchange correlation	LDA	LDA	GGA	
Lattice constant (Å)	5.877	5.6591[a] , 5.8509[b]	6.014[b], 5.946[c], 5.994[d]	5.861[e], 5.868[f]
Energy band-gap (eV)	0.55	0.564[b]	0.2674[b], 0.84[d]	1.424[g], 1.46[h]

[a]Ref. [28], [b]Ref. [29], [c]Ref. [30], [d]Ref. [31], [e]Ref. [32], [f]Ref. [33], [g]Ref. [34], [h]Ref. [35]

It is found that variation in the bond lengths with respect to bulk bond length (2.54 Å) is more for surface atoms compared to core atoms. Further bond length variation is larger for (111) phased NW compared to other two phases of NW. Variation in In-P bond length also results in change in the bond angle. P-In-P and In-P-In bond angle changes from ideal value of 109.42° to an average of 118.56°, 114.89°,113.6° for P-In-P and 105.28°, 104.32°,103.44° for In-P-In along (100), (110), and (111) phases respectively. The observed values are approximately 5.72% larger and 4.64% smaller compared to ideal case for P-In-P and In-P-In respectively. Thus, it is noticed that bond length and bond angles for core region of NWs exhibit smaller

variation as compared to outer region. Surface atom optimize such that cation (anion) atoms move slightly inward (outward) in contrast to their unoptimized position. Similar findings were also reported by Carter *et al.* [**36**] on GaN NWs and Alves *et al.* [**37**] on III-V semiconductor surfaces.

To compare the structural stabilities of the considered NWs, we calculate the binding energy (BE) per In-P pair for different phases and summarized the findings in Table 2. BE is calculated as

$$BE = \frac{E_{Total}}{n} - E_{In} - E_P \qquad (1)$$

where, in Eq. (1) E_{Total}, E_{In}, E_P and are the total energies of NWs structure, isolated In and P atom respectively, n is number of In - P pairs present in the NWs. It can be clearly seen in the **Table 2** that BE changes as the phases of NW changes. However, these values are smaller than the BE for bulk InP (-3.47 eV), which means stability of NWs is lesser than bulk InP. From **Table 2**, it can be deduced that (100) phased NWs are energetically more favourable than other two crystallographic phases. Further, NWs in (111) phase exhibits least negative BE making this particular phase thermodynamically less stable than rest of the two phases.

**Table 2.** Calculated Binding energy per In-P pair (BE) of NWs phases.

NWs Phases	BE (eV)
(100)	-2.78
(110)	-2.67
(111)	-2.59

To analyze the electronic properties of optimized NW structure, we investigate band structure and density of states (DOS) profile of considered NWs. Band structures are depicted in **Fig. 3(a), (b)** and **(c)**. From **Fig. 3 (a)** it is revealed that NWs directed along (100) phase are semiconductor with band-gap of 0.71 eV.
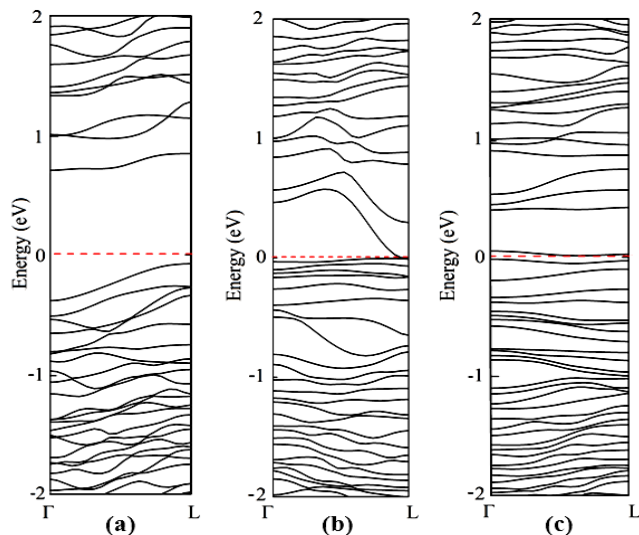
Fig. 3. Band Structures of NW in (a) (100), (b) (110), (c) (111) phases. The Fermi level is set at 0 eV as shown by dashed line.

As valance band maximum (VBM) and conduction band minimum (CBM) are located at different symmetry points of the Brillouin-zone, indicating the indirect nature of band-gap. Further NW in (110) phase exhibits metallic behaviour due to localization of energy state across the Fermi level [**Fig. 3 (b)**]. Also, (111) phased NW becomes semi-metallic [**Fig. 3 (c)**] in nature. For further detailed analysis, we calculate the total density of states (DOS) and projected density of states (PDOS) near the Fermi level.
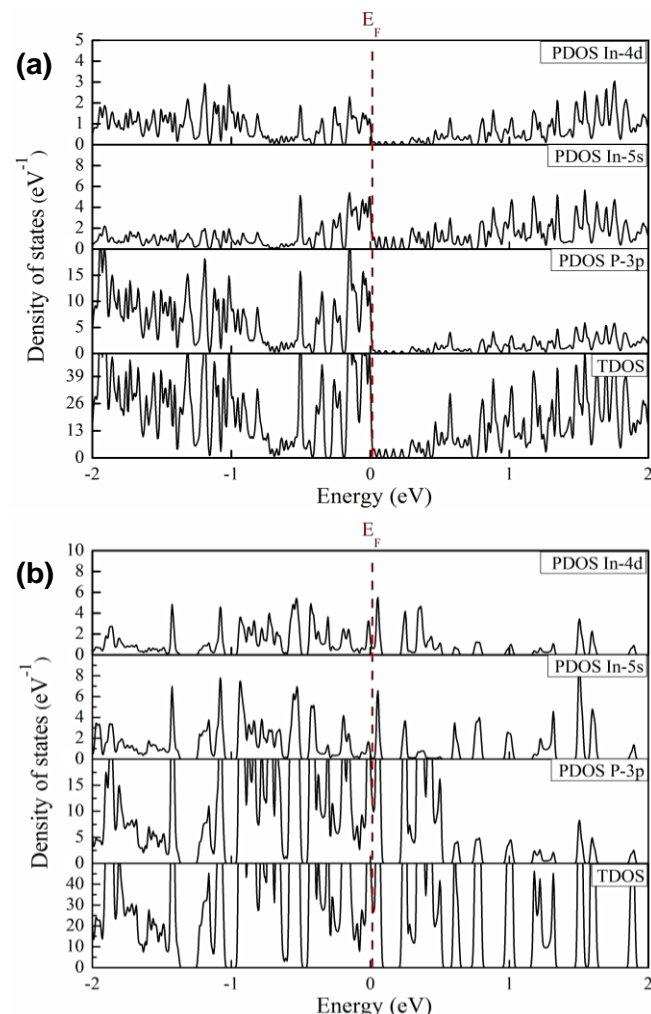
Fig. 4. TDOS and Partial DOS of NW in (a) (110) phase, (b) (111) phase.

Since DOS profile for NWs along (100) phase are trivial as they exhibit a non-available electronic states across the Fermi level, therefore, to be concise this DOS profile is not presented. DOS profile of NW along (110) and (111) phases are depicted in **Fig. 4 (a)** and **Fig. 4 (b)**. The computed DOS plots for (110) phase NW as shown in **Fig. 4 (a)** highlights a large availability of electronic states across the Fermi level. Such large magnitude of electronic peaks across the Fermi level indicates its metallic nature. The PDOS analysis revealed that P *3p* electrons are having major contribution towards the states near the Fermi level with a minor contribution from In *4d* and In *5s* electrons. The DOS plot for (111) phase NW as depicted in **Fig. 4 (b)** shows the existence of a number of sharp peaks in the valence as well as in the conduction band near the Fermi

level. Further, in a closer observation we find few states just at the Fermi level together with few prominent peaks in the conduction band near the Fermi level. This supports the semi-metallic behavior of the configuration as observed in the corresponding band structure [**Fig. 3** (**c**)]. The analysis of PDOS suggests that majority of the electronic states in the vicinity of Fermi level are governed by the P *3p* electrons with a minor contribution of In *4d* and In *5s* electrons **[Fig. 4 (b)]**.

Conclusion

Conclusively, DFT based *ab-initio* calculation highlights structural stability and electronic properties of NW are dependent on crystallographic phase of NWs. The BE calculation shows that stability of NWs is strongly phase dependent and the most energetically stable structure is directed along (100) phase. NW directed along (111) phase having least stable BE and exhibit semi-metallic nature. NW directed along (100) phase exhibit semiconducting behavior whereas (110) phased NW exhibit metallic nature. We therefore conclude that the energetic of Zinc-blende InP NWs is strongly dependent on the selection of particular crystallographic phases. The dependency of energetic of NW on the phases of structural may be useful in many electronic and optical applications.
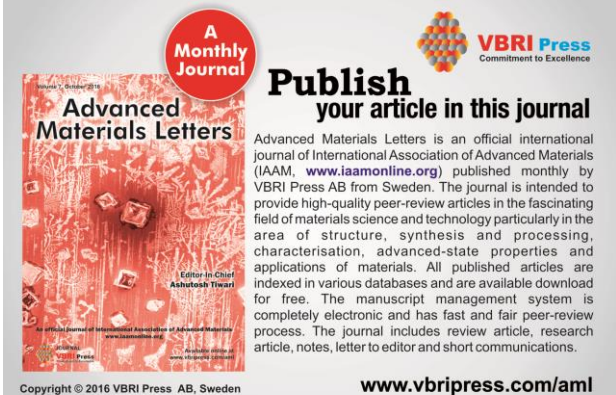
References

1. Gudiksen, M. S.; Lauhon, L. J.; Wang, J., Smith; D. C., Lieber, C. M.; *Nature,* **2002**, *415*, 617.
    DOI: 10.1038/415617a
2. Duan, X.; Huang, Y.; Cui, Y.; Wang, J.; Lieber, C. M.; *Nature,* **2001**, *409*, 66.
    DOI: 10.1038/35051047
3. Huang, Y. ; Duan, X.; Cui, Y.; Lauhon, L. J.; Kim, K H.; Lieber, C. M.; *Science*, **2001**, *294*, 1313.
    DOI: 10.1126/science.1066192
4. Cui, Y. ; Zhong, Z.; Wang, D.; Wang, W. U.; Lieber, C. M.; *Nano lett.,* **2003**, *3,* 149.
    DOI: 10.1021/nl0258751
5. Colinge, J-P. ; Lee, C-W.; Afzalian, A. ; Akhavan, N. D.; Yan, R.; Ferain, I.; Razavi, P.; O'Neill, B; Blake, A.; White, M.; Kelleher, A-M; McCarthy, B; Murphy, R.; *Nature Nanotechnology,* **2010**, *5,* 225.
    DOI: 10.1038/nnano.2010.15
6. Li, Y.; Qian, F.; Xiang, J. ; Lieber, C. M.; *Materials Today,* **2006**, *9,* 18.
    DOI: 10.1016/S1369-7021(06)71650-9
7. Patolsky, F.; Lieber, C. M.; *Materials Today,* **2005**, *8*, 20.
    DOI: 10.1016/S1369-7021(05)00791-1
8. Hsueh, T. J.; Hsu, C. L.; Chang, S-J.; Chen, I-C.; *Sens. Actuators, B,* **2007**, *126,*473.
    DOI: 10.1016/j.snb.2007.03.034
9. Novotny, C. J.; Yu, E. T.; Yu, P. K. L.; *Nano Lett.,* **2008**, *8,* 775.
    DOI: 10.1021/nl072372c
10. Lai, E.; Kim, W.; Yang, P.; *Nano Research,* **2008**, *1*, 123.
    DOI: 10.1007/s12274-008-8017-4
11. Mohan, P.; Motohisa, J.; Fukui, T.; *Nanotechnology,* **2005**, *16*, 2903.
    DOI: 10.1088/0957-4484/16/12/029
12. Gudiksen, M. S.; Wang, J.; Lieber, C. M.; *J. Phys. Chem. B,* **2001**, *105,* 4062.
    DOI: 10.1021/jp010540y
13. Fanfai, D. D.; Korgel, B. A.; *Cryst. Growth Des.,* **2005**, *5,* 1971.
    DOI: 10.1021/cg0502587
14. Yang, Q.; Tang, K.; Li, Q.; Yin, H.; Wang, C.; Qian, Y.; *Nanotechnology,* **2004**, *15*, 918.
    DOI: 10.1088/0957-4484/15/8/008
15. Joyce, H. J.; Leung, J. W.; Gao, Q.; Tan, H. H.; Jagadish, C.; *Nano lett.,* **2010**, *10,* 908.
    DOI: 10.1021/nl903688v
16. Zhao, Y.; Yu, Y.; Gao, F.; *Journal of Crystal Growth,* **2013**, *371,* 148.
    DOI: 10.1016/j.jcrysgro.2013.02.018
17. Santos, C. L. D.; Piquini, P.; *Phys. Rev. B,* **2010**, *81,* 075408.
    DOI: 10.1103/PhysRevB.81.075408
18. Sano, K.; Akiyama, T.; Nakamura, K.; Ito, T.; *Journal of Crystal Growth,* **2007**, *301,* 862.
    DOI: 10.1016/j.jcrysgro.2006.11.325
19. Akiyama, T.; Nakamura, K.; Ito, T.; *Phys. Rev. B: Condens. Matter Mater. Phys.,* **2006**, *73,* 235308.
    DOI: 10.1103/PhysRevB.73.235308
20. Leitsmann, R.; Bechstedt, F.; *Journal Applied. Physics,* **2007***, 102,* 063528.
    DOI: 10.1063/1.2783899
21. Gadret, E. T.; Dias, G. O.; Dacal, L. C. O.; de Lima, M. M.; Ruffo, C. V. R. S.; Iikawa, F.; Brasil, M. J. S. P.; Chiaramonte, T.; Cotta, M. A.; Tizei, L. H. G.; Ugarte, D.; Cantarero, A.; *Phys. Rev. B: Condens. Matter Mater. Phys.,* **2010**, *82*, 125327.
    DOI: 10.1103/PhysRevB.82.125327
22. Yamashita, T.; Akiyama, T.; Nakamura K.; Ito, T.; *Jpn. J. Appl. Phys.,* **2010**, *49*, 055003.
    DOI: 10.1143/JJAP.49.055003
23. Georg, K.; Hafner, J.; *Phys. Rev. B: Condens. Matter Mater. Phys,* **1993**, *47*, 558.
    DOI: 10.1103/PhysRevB.47.558
24. Georg K.; Furthm¨uller, D.; *Phys. Rev. B: Condens. Matter Mater. Phys.,* **1996**, *54*, 11169.
    DOI: 10.1103/PhysRevB.54.11169
25. Perdew, J. P.; Zunger, A.; *Phys. Rev. B: Condens. Matter Mater. Phys.,* **1981**, *23*, 5048.
    DOI: 10.1103/PhysRevB.23.5048
26. Georg, K.; Joubert, D.; *Phys. Rev. B: Condens. Matter Mater. Phys.,* **1999**, *59*, 1758.
    DOI: 10.1103/PhysRevB.59.1758
27. Monkhorst, H. J.; Pack, J. D.; *Phys. Rev. B: Condens. Matter Mater. Phys.,* **1976**, *13*, 5188.
    DOI: 10.1103/PhysRevB.13.5188
28. Karazhanov, S. Z.; Lew Yan Voon, L. C.; *Semiconductors,* **2005**, *39,* 161.
    DOI: 10.1134/1.1864192
29. Ameri, M.; Bentouaf, A.; Doui-Aici, M.; Khenata, R.; Boufadi, F.; Touia, A.; *Materials Sciences and Applications,* **2011**, *2,* 729.
    DOI: 10.4236/msa.2011.27101
30. Dacal, L. C. O.; Cantarero, A.; *Solid State Commun.,* **2011**, *151*, 781.
    DOI:10.1016/j.ssc.2011.03.003
31. Shan, D.; Feng, Z.; *Chinese Physics B,* **2012**, *21*, 097502.
    DOI: 10.1088/1674-1056/21/9/097502
32. Bimberg, D.; Blachnik, R.; Cardona, M.; Dean, P.J.; Grave, T.; Harbeke, G.; Hübner, K.; Kaufmann, U.; Kress, W.; Madelung, O.; Münch, W. von; Rössler, U.; Schneider, J.; Schulz, M.; Skolnick, M.S.; Madelung, O. (Eds); Semiconductors, Physics of Group IV Elements and III-V Compound, 1st ed.; Springer: Berlin, **1982**.
33. Sze, S. M.; Physics of Semiconductor Device; Wiley: New York, **1981**.
34. Wyckoff, R. W. G.; Crystal Structures, 1st ed.; Krieger: Malabar, **1986**.
35. Madelung, O.; Semiconductors: Data Handbook,3rd ed.; Springer: Berlin, **2004**.
    DOI: 10.1007/978-3-642-18865-7
36. Carter, D.J.; Gale, J.D.; Delley B.; Stampfl, C.; *Phys. Rev. B: Condens. Matter Mater. Phys.,* **2008**, *77*, 115349.
    DOI: 10.1103/PhysRevB.77.115349

37. Alves, J. L. A.; Hebenstreit, J.; Scheffler, M; *Phys. Rev. B: Condens. Matter Mater. Phys.,* **1991**, *44*, 6188.
    DOI: 10.1103/PhysRevB.44.6188